Static Characteristics of a New Doubly Salient Permanent Magnet Motor

Ming Cheng, K.T.Chau and C.C.Chan
Department of Electrical and Electronic Engineering, The University of Hong Kong, Pokfulam Road, Hong Kong

Abstract – In this paper, magnetic field analysis of a new doubly salient permanent magnet (DSPM) motor is carried out based on finite element method (FEM). Hence, the corresponding static characteristics, including PM flux-linkage, self-inductance and mutual-inductance, are deduced (the interaction between PM field and armature field are taken into account). A method for measuring the motor inductance is newly proposed. The theoretical analysis is verified by experimental results.

I. INTRODUCTION

Recent developments of the doubly salient permanent magnet (DSPM) motor have shown that it has many advantages such as high efficiency, high power density and high energy conversion ratio [1]-[3]. Thus, more and more attention has been paid to this motor since its appearance. However, the static characteristics of the motor, being the basis in the performance prediction and control, have received insufficient research. The PM flux linkage and phase inductance in the available literatures are obtained under the assumptions that the variations of the PM flux linkage and the armature reaction flux linkage are spatially dependent only [2]. In addition, the corresponding mutual inductance has never been mentioned.

The objective of this paper is to propose the analysis of the magnetic field distribution of the DSPM motor by using finite element method, and to calculate the PM flux linkage and phase inductance. The iron saturation and the cross-coupling between the PM flux and armature flux are taken into consideration. A new 6/4 pole DSPM motor with stationary PMs is designed, built and tested for exemplification. The experimental results verify the theoretical analysis.

II. MAGNETIC FIELD ANALYSIS

Two dimensional (2D) finite element analysis is used to determined the magnetic field distribution of the DSPM motor. The magnetic field prevailing in the interior of the machine can be described in terms of the vector potential. In a 2D rectangular coordinate, the nonlinear magnetostatic Poisson equation is given by:

$$\begin{cases} \dfrac{\partial}{\partial x}(\nu\dfrac{\partial A_z}{\partial x})+\dfrac{\partial}{\partial y}(\nu\dfrac{\partial A_z}{\partial y})=-(J_z+J_c) \\ S_1+S_2: A_z=0 \end{cases} \quad (1)$$

where A_z and J_z are the z components of vector potential $\vec{A}$ and current density $\vec{J}$, respectively. J_c is the equivalent surface current density of the permanent magnet. s_1 and s_2 denote the Dirichlet boundary.

Fig. 1 shows the schematic configuration of the DSPM motor. Due to the semiperiodic motor configuration, the region of interest for finite element analysis is a half of the whole motor cross section. Fig. 2 shows the finite element mesh of this motor. Fig. 3 shows the flux distributions under no-load and load conditions with rotor angle of 30° (the rotor angle is defined as the angle between the central lines of stator pole and rotor slot; the rotor angle is zero as the stator pole central line aligns with the rotor slot central line). The corresponding magnetic flux density distributions in the air-gap are shown in Fig. 4. It can be seen that the flux in the DSPM motor is mainly contributed by PM. The armature flux has less effect on the total flux value, but it changes the flux distribution.

III. PM FLUX LINKAGE

The PM flux linkage versus rotor angle can be obtained from the finite element analysis as shown in Fig. 5. The induced back EMF is given by:

$$e=\frac{d\psi_m}{dt}=\frac{d\psi_m}{d\theta}\cdot\frac{2\pi n}{60} \quad (2)$$

The waveform of the EMF is given in Fig. 6. It can be seen that the experimental result agrees with the theoretical one (not only in the waveform shape, but also in the peak value).

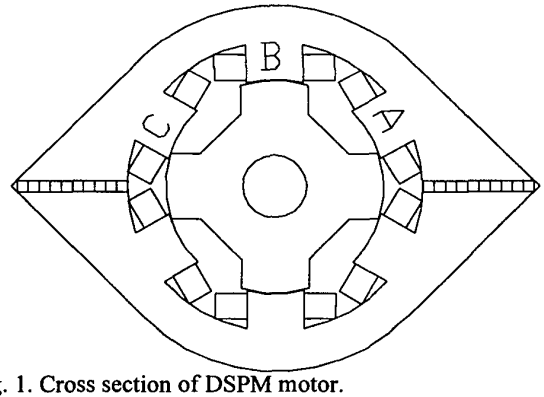

Fig. 1. Cross section of DSPM motor.

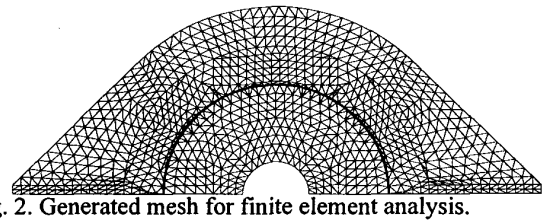

Fig. 2. Generated mesh for finite element analysis.

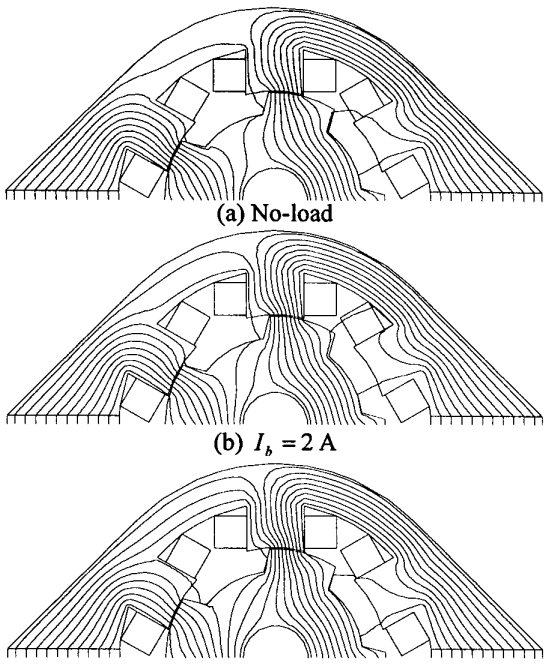

(a) No-load

(b) $I_b = 2$ A

(c) $I_b = 2$ A, $I_c = -2$ A

Fig. 3. Flux distributions under different conditions.

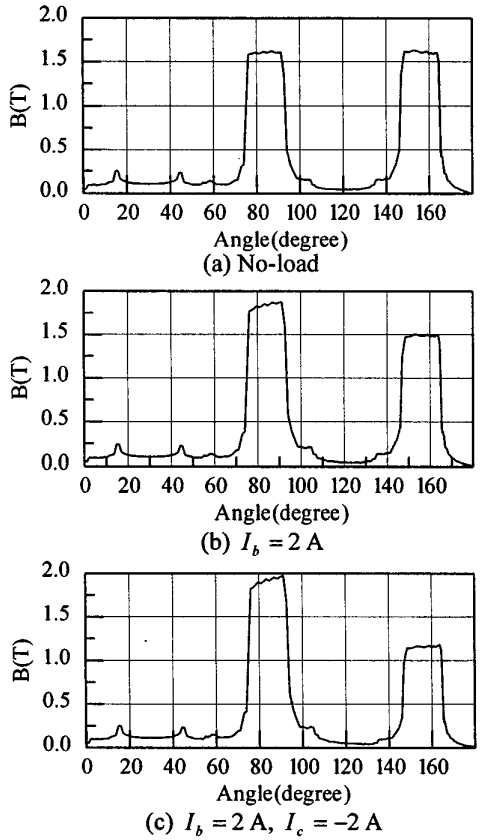

(a) No-load

(b) $I_b = 2$ A

(c) $I_b = 2$ A, $I_c = -2$ A

Fig. 4. Magnetic flux density in air-gap ($\theta_b = 30°$).

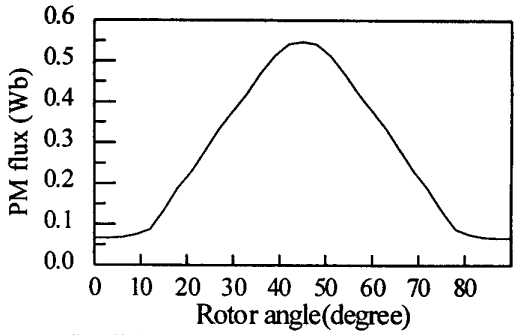

Fig. 5. PM flux linkage versus rotor angle.

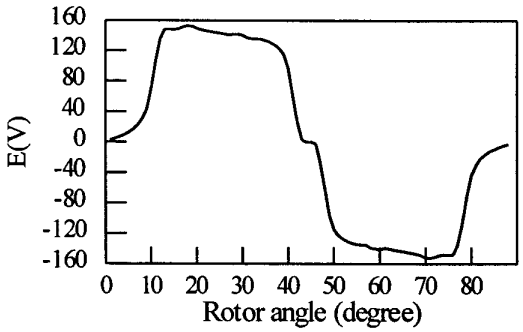

(a) Theoretical

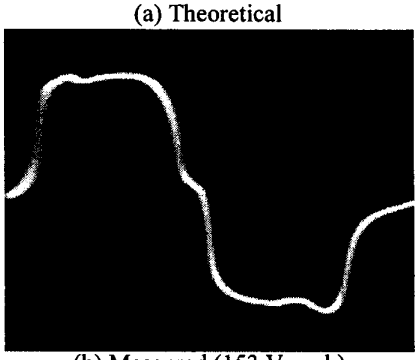

(b) Measured (153 V peak)

Fig. 6. Back EMF waveforms.

IV. INDUCTANCES

In the calculation of inductances, the cross-coupling between the PM flux and armature flux should be considered. As the PM and armature current act together, the flux linkage of one phase is given by:

$$\psi = \psi_m + Li \tag{3}$$

where ψ_m is the PM flux linkage at no-load. Then, the inductance should be expressed as:

$$L = \frac{\psi - \psi_m}{i} \tag{4}$$

Fig. 7 (a) shows the self-inductance characteristics. It indicates that the self-inductances with and without PM are much different in both value and pattern. In addition, the strengthening and weakening actions of armature field to PM field have significant effect on the inductance value, which

should be taken into account in performance prediction and control of the DSPM motor. From Fig. 7 (b), it is seen that the DSPM motor has a large mutual inductance, similar level as the self-inductance. Its peak value occurs at the position that the stator pole and rotor pole are half overlapped.

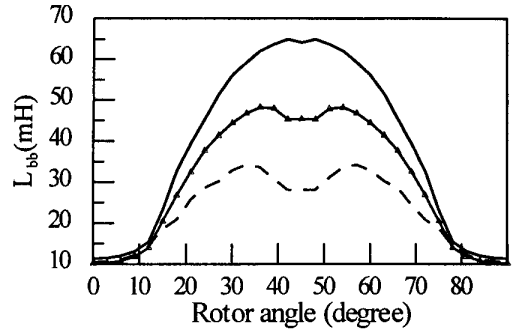

(a) Self-inductance

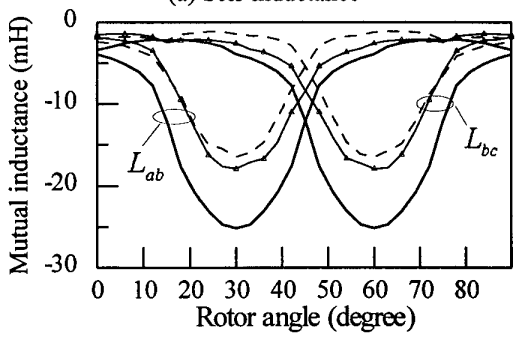

(b) Mutual inductance

Fig. 7. Phase inductances versus rotor angle.

V. INDUCTANCE MEASUREMENT

As shown in Fig. 8, p is the operating point at no-load. As a sinusoidal measuring voltage is applied to a phase winding, a sinusoidal component of flux is added to ϕ_0. The peak values of voltage and flux have following relationship:

$$U_m \approx E_m = \omega N \phi_{\max} \tag{5}$$

where N is the series turns per phase. When the peak values of voltage and current are measured, the inductances are:

$$L^+ = \frac{N\phi_{\max}}{i^+_{\max}} = \frac{U_m}{\omega i^+_{\max}}, \quad L^- = \frac{N\phi_{\max}}{i^-_{\max}} = \frac{U_m}{\omega i^-_{\max}} \tag{6}$$

As seen from Fig. 8, $i^+_{\max} > i^-_{\max}$, so $L^+ < L^-$. If the rms values of voltage and current as well as the input power are measured, then the average value of self-inductance can be approximately obtained as:

$$L = \frac{1}{\omega} \frac{b}{g^2 + b^2} \tag{7}$$

where $g = I_g / U$, $b = I_u / U$, I_g and I_u are the real and imaginary components of the current, respectively. Table I shows the comparison of the calculated inductances and the measured ones at two rotor positions. As expected, a good agreement is found.

TABLE I. COMPARISON OF SELF-INDUCTANCES AT 2.5 A.

θ (°)	L^+ (mH)	L^- (mH)	Calculated (mH)	Measured (mH)
15	18.24	20.49	19.37	20.5
45	26.83	47.14	36.99	39.8

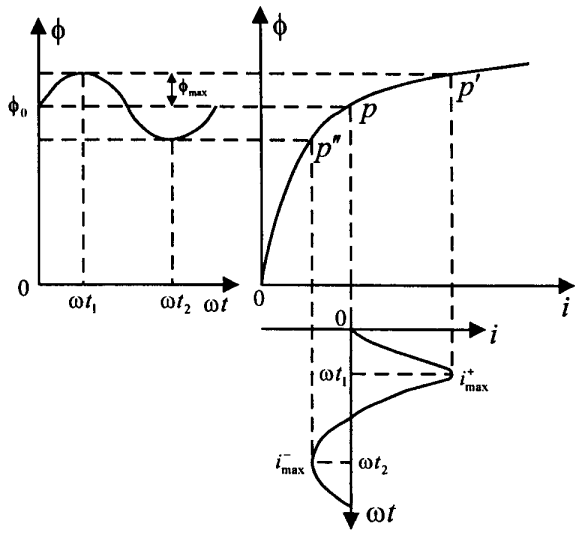

Fig. 8. Current waveform under sinusoidal flux.

VI. CONCLUSION

The magnetic field and static characteristics of a new DSPM motor have been presented, showing that the magnetic flux density distribution is manly contributed by PM, the cross-coupling between PM flux and armature flux has significant effect on the inductance, and the corresponding mutual inductance should not be neglected. The measurement method for the self-inductance has also been discussed. The experimental results verify the proposed theoretical analysis.

VII. ACKNOWLEDGMENT

This work was supported and funded in part by the Committee on Research and Conference Grants of the University of Hong Kong, the Hong Kong Research Grants Council, and the National Natural Science Foundation of China (Project 59507001).

VIII. REFERENCES

[1] S. Huang, J. Luo, F. Leonardi and T.A. Lipo, "A general approach to sizing and power density equations for comparison of electrical machines," IEEE Trans. Industry Application, Vol. 34, pp. 92-97, 1998.

[2] Y. Liao, F. Liang and T.A. Lipo, "A novel permanent magnet motor with doubly salient structure," IEEE Trans. Industry Applications, Vol. 31, pp. 1069-1078, 1995.

[3] M. Cheng, K.T. Chau and C.C. Chan. "A new doubly salient permanent magnet motor," IEEE PEDES'98 Proc., 1998.